

RECEIVED: December 10, 2023

REVISED: February 22, 2024

ACCEPTED: May 16, 2024

PUBLISHED: June 4, 2024

LIGHT DETECTION IN NOBLE ELEMENTS (LIDINE 2023)

MADRID, SPAIN

20–22 SEPTEMBER 2023

## **$^{37}\text{Ar}$ source on-demand production and deployment for low-energy nuclear recoil measurement in ReD liquid Argon TPC**

---

**P. Zakhary on behalf of the DarkSide collaboration**

*AstroCeNT, Nicolaus Copernicus Astronomical Center of the Polish Academy of Sciences,  
Warsaw, Poland*

*E-mail:* [pzakhary@camk.edu.pl](mailto:pzakhary@camk.edu.pl)

**ABSTRACT.** The search for light dark matter ( $< 10 \text{ GeV}/c^2$ ) has become increasingly important, since no conclusive evidence has been found in the higher dark matter (DM) mass region. In order to explore this light mass range, it is necessary to accurately model the response of the noble liquid time projection chamber (TPC) detectors, used in many experiments aimed at the direct measurement of DM, to low energy ( $< 1 \text{ keV}$ ) nuclear recoils (NRs). In this respect,  $^{37}\text{Ar}$  provides an ideal calibration source in the low-energy region due to its two low-energy peaks at 0.27 and 2.82 keV following electron capture with a 35-day half-life. We propose a method to produce  $^{37}\text{Ar}$  without chemical or heating treatments by using the  $^{40}\text{Ca}(\text{n},\alpha)^{37}\text{Ar}$  reaction. This can be achieved by irradiating nano-CaO powder with a neutron source (e.g. AmBe) and allowing the produced  $^{37}\text{Ar}$  to diffuse into the argon used inside a double-phase TPC. By measuring the NR yields relative to those two low-energy points in the Recoil Directionality (ReD) experiment, other detectors can be cross-calibrated with the same source deployed. In this talk, the  $^{37}\text{Ar}$  source production, its deployment, and preliminary results will be presented.

**KEYWORDS:** Dark Matter detectors (WIMPs, axions, etc.); Time projection chambers

2024 JINST 19 C06003



© 2024 The Author(s). Published by IOP Publishing Ltd on behalf of SISSA Medialab. Original content from this work may be used under the terms of the [Creative Commons Attribution 4.0 licence](#). Any further distribution of this work must maintain attribution to the author(s) and the title of the work, journal citation and DOI.

<https://doi.org/10.1088/1748-0221/19/06/C06003>

---

## Contents

<b>1</b>	<b>Low-mass dark matter searches in liquid argon TPC</b>	<b>1</b>
<b>2</b>	<b><math>^{37}\text{Ar}</math> source: a “standard candle” in the low-energy calibration</b>	<b>2</b>
<b>3</b>	<b><math>^{37}\text{Ar}</math> source: calibration campaign</b>	<b>3</b>
3.1	On-demand production	3
3.2	Data analysis	4
<b>4</b>	<b>Conclusions</b>	<b>5</b>

---

## 1 Low-mass dark matter searches in liquid argon TPC

Advancements in the field of Astroparticle physics have always hinged on the development of sensitive experiments aimed at detecting elusive natural phenomena. Despite many evidence spanning diverse cosmological scales substantiating the *existence* of dark matter (DM), its *nature* i.e. its precise microphysical properties, remains undetermined. Consequently, a concerted effort is underway to detect Weakly Interacting Massive Particles (WIMPs), a widely supported candidate for DM, through the deployment of various technologies. These technologies are designed to detect very low energy deposits resulting from the direct interaction of these enigmatic particles with the target material of the experiment, e.g. liquefied noble gases or solid crystals [1–5].

The pursuit has already narrowed down the parameter space of WIMPs with masses  $\mathcal{O}(10\,\text{GeV}/c^2)$  and cross-sections of  $\mathcal{O}(10^{-45}\,\text{cm}^2)$ . Presently, the research is progressing towards lower masses of  $\mathcal{O}(\text{few GeV}/c^2)$ . For liquid noble gas detectors, this entails less energetic recoils i.e. the sensitivity requirement transitions from 20–100 keV to  $\mathcal{O}(\text{few keVs})$ , particularly in the case of Liquid Argon (LAr) [6, 7]. The focus is not only on sensitivity to the low-energy recoils but also on the ability to distinguish these interactions from other background signals in the surrounding environment generated by different particles.

In a dual-phased time projection chamber (TPC) utilizing liquefied noble gases, any energy deposited in the target volume is divided between the excitation and ionization channels. Current experiments employing this technology leverage the excitation and ionization channels to generate observable signals, which are then detected by photosensors. The electron-ion recombination process critically determines the allocation between these two potential channels, namely the primary scintillation photons (S1) and the extracted electrons (S2). The reconstruction of these two signals provides valuable information, including the 3D event position: the (Z) position is derived from the drift time between the S1 and S2 signals, while the (XY) position is inferred from the light pattern of the S2. Furthermore, this approach enables pulse shape discrimination (PSD) between the expected signals from WIMPs, namely, nuclear recoils (NRs), and  $\beta$  and  $\gamma$ -rays that produce electron recoils (ERs), constituting the majority of the background.

## 2 $^{37}\text{Ar}$ source: a “standard candle” in the low-energy calibration

To achieve precision in calibrating the LAr response, the utilization of  $^{37}\text{Ar}$  emerges as a strategic choice within the low-energy spectrum, distinguished by discernible peaks at 0.27 and 2.82 keV subsequent to electron capture, and characterized by a 35-day half-life, i.e. it would soon decay naturally once the calibration has been completed.  $^{37}\text{Ar}$  can be produced through different reactions; namely  $^{36}\text{Ar}(\text{n},\gamma)^{37}\text{Ar}$ ,  $^{37}\text{Cl}(\text{p},\text{n})^{37}\text{Ar}$ , or  $^{40}\text{Ca}(\text{n},\alpha)^{37}\text{Ar}$ . The first reaction has been used in [8]. The second reaction necessitates access to a proton beam facility and has been applied in the studies outlined in [9, 10]. Investigations conducted by [11–13] predominantly relied on the final reaction. Nonetheless, a recurring challenge associated with this reaction lies in the extraction of  $^{37}\text{Ar}$  from the matrix, typically involving chemical or thermal treatments.

There is another possibility reported in [14] that  $^{37}\text{Ar}$  can be produced from nano-CaO as a gas phase radionuclide by irradiation in vacuum. This suggests the possibility of liberation from nano-CaO without chemical or heating interventions. Therefore, our proposed on-demand methodology involves irradiating nano-CaO powder with a neutron source, and facilitating the diffusion of the resulting  $^{37}\text{Ar}$  into the argon within the TPC via a gas circulation system. Notably, a similar approach was implemented in a spherical gaseous detector utilizing calcium salt powder [15].

Given the current interest in low-mass WIMPs searches, it’s important to quantify NR yields in LAr relative to low-energy benchmarks, such as  $^{37}\text{Ar}$ , in order to cross-calibrate prospective detectors. Notably the current lowest direct measurement in LAr is 6.7 keV $_{nr}$  [16].



**Figure 1.** *Left:* the nano-CaO powder container next to the Am-Be source inside a PE shielding. *Right:* after irradiation, the container inside the HPGe detector to examine the associated  $^{42}\text{K}$  production.

By employing PHITS Monte Carlo (MC) simulation [17], we assessed irradiating 40 g of nano-CaO powder with the INFN-LNS Am-Be source (34 GBq,  $2.2 \times 10^6$  neutrons/s). This simulation resulted in the production of 100 Bq of  $^{37}\text{Ar}$  during a 10-day irradiation period. Another factor to be considered here is the relative proportion of LAr volume enclosed by the TPC to the total liquid argon volume within the system, with the chamber constituting 3% of the latter. Therefore we can anticipate the detectability of 3 Bq of  $^{37}\text{Ar}$  within the TPC in case of 100% extraction efficiency.

Our efforts encompassed the preparation of the  $^{37}\text{Ar}$  source, the irradiation was conducted at INFN-LNS. The irradiation occurred within a PE shielding in the “Hot Room” at INFN-LNS and lasted for 18 days and 23 hours till the system is ready, see figure 1.

Additionally, an indirect assessment of  $^{37}\text{Ar}$  yield through the examination of associated  $^{42}\text{K}$  production has been performed. This auxiliary measurement was done with the assistance of INFN-LNS experts and the use of the available HPGe detector, as shown in figure 1.  $^{42}\text{K}$ , one of the byproducts of the activation process, was observed with  $2.9 \pm 0.5 \text{ Bq}$ . Based on the simulation, this implied that  $^{37}\text{Ar}$  should have been activated conservatively with  $O(10^2) \text{ Bq}$ . Nevertheless, to mitigate complete dependence on the HPGe measurements, given some of their inherent uncertainties, we can assert, albeit without precise quantification, that the activation of  $^{37}\text{Ar}$  has *at least* taken place as anticipated in the simulation.

### 3 $^{37}\text{Ar}$ source: calibration campaign

$^{37}\text{Ar}$  is released spontaneously as a gaseous radio-nuclide post-irradiation. To transfer  $^{37}\text{Ar}$  to a radiochemically clean receptacle, such as the TPC, can theoretically be accomplished by allowing it to diffuse out due to a pressure gradient, while preserving the integrity of the irradiated nano-CaO powder. Consequently, we configured Swagelok components to house the nano-powder, as depicted in figure 2.

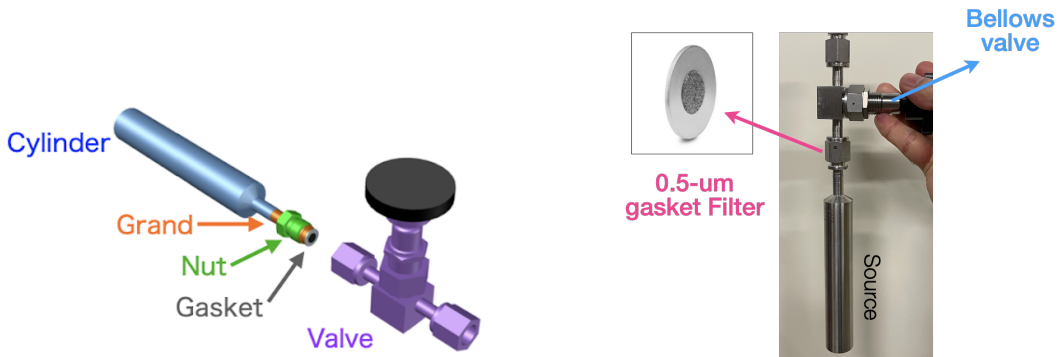


**Figure 2.** The left diagram depicts Swagelok components housing CaO nano-powder, while the right image emphasizes the actual container, spotlighting the  $0.5 \mu\text{m}$  gasket filter and the bellows valve linking the container to the gas panel.

Initial trials were conducted in collaboration with experts from INFN-LNS, utilizing a setup comprising a dry pump, a turbo pump, a pressure gauge, a scale, and various types of valves. Employing the dry pump, we achieved a vacuum of  $8 \times 10^{-2} \text{ mbar}$  with an average pumping rate of approximately  $1 \text{ mbar}/8 \text{ sec}$ . Subsequently, we explored the combination of the dry pump with the Pfeiffer HiCube 80 Turbo Pumping Station, achieving a plateau of  $6.9 \times 10^{-4} \text{ mbar}$  after 3 hours of pumping, which remained stable overnight with minimal fluctuations.

#### 3.1 On-demand production

The irradiation procedure commenced with the addition of 40 grams of nano-CaO powder into the container. The remaining volume was then vacuumed and filled with Ar (class-6) gas at a pressure of 1.2 bar. The irradiation process utilized the Am-Be source as described in section 2. The Gas Panel is illustrated in figure 3. The vacuuming process along the line (between HV107 and HV110) was initiated through HV111, with the CaO container valve closed. The vacuuming process reached a pressure of  $7 \times 10^{-2} \text{ mbar}$ . Subsequently, the HV111 valve was opened which resulted in a pressure of  $6 \times 10^{-2} \text{ mbar}$ .

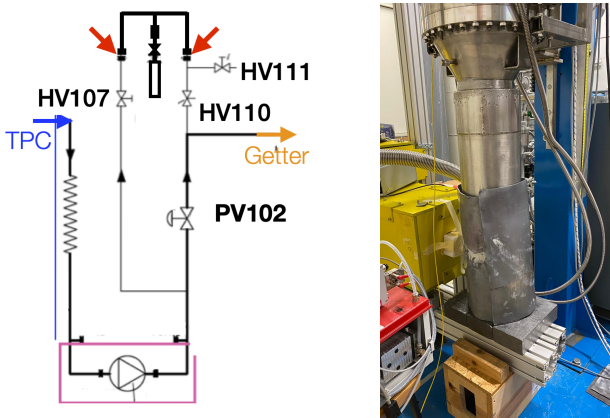


**Figure 3.** The left schematic of the gas panel delineates the  $^{37}\text{Ar}$  calibration loop in relation to the gas conduit supplying the TPC (indicated by a blue arrow) and the pipe leading to the purification system “Getter” (indicated by an orange arrow). The  $^{37}\text{Ar}$  source bottle is connected in between the red arrows. On the right side, the image portrays the cryostat containing the TPC shielded with lead during data acquisition.

Following this step, HV111 was closed, and the vacuuming of the line was stopped. The valve above the CaO holder was then opened, allowing the gas within the holder to be extracted to the gas panel located between HV107 and HV110. Subsequently, after some time enough for diffusing the generated  $^{37}\text{Ar}$  out of holder to the gas conduit feeding the TPC, the valve was closed.

The sequential opening of HV107 and HV110, coupled with the closure of PV102, caused a decrease in pressure within the gas panel from 1860 to 1830 mbar. At this point, the Ar gas from the gas panel was intended to propel the  $^{37}\text{Ar}$  inside the system. Upon closing HV107 and HV110 and opening PV102, the entire source loop was excluded, resulting in an increase in pressure within the gas panel from 1830 to 1860 mbar.

### 3.2 Data analysis

We took data for 6.5-hour before  $^{37}\text{Ar}$  injection for background and for 2.5 hours after the  $^{37}\text{Ar}$  diffusion into the TPC in the same DAQ conditions in “S2-trigger” Mode. In this mode, the trigger fires on S2 pulse since S1 from  $^{37}\text{Ar}$  event is too small to be triggered efficiently. Waveforms were recorded with 88  $\mu\text{s}$  time window, with post trigger size of 27% (i.e.  $[-64.24, +23.76] \mu\text{s}$ ). Coincidence of three SiPMs among the top inner eight SiPMs was required within 2032 ns. This DAQ configuration achieved a target threshold of 15 ADC, approximately 0.5 PE. A series of tests on the DAQ system was conducted, culminating in the successful establishment of a triggering scheme tailored for low energy thresholds. This achievement was validated through its application to  $^{83m}\text{Kr}$  data utilizing the S2-trigger mode, demonstrating efficacy with a threshold around 1 PE level. The cryostat hosting the TPC was shielded with a layer of lead surrounding it and beneath it to suppress the accidental event rate. An event is considered if there is at least a 5 ms delay from the previously triggered event. We applied fiducialization looking only at events happening in the inner 2 cm of the TPC.

The analysis can neither confirm nor reject the observation of  $^{37}\text{Ar}$ . Assuming 100% liberation efficiency of  $^{37}\text{Ar}$  from the CaO holder, MC expected  $^{37}\text{Ar}$  activity to be 0.5 Bq in the final sample of events incorporating all quality cuts. This corresponds to 8 counts/hour/PE for the k-shell peak. Since this is on the limit of our system sensitivity, we report the observed spectrum before and

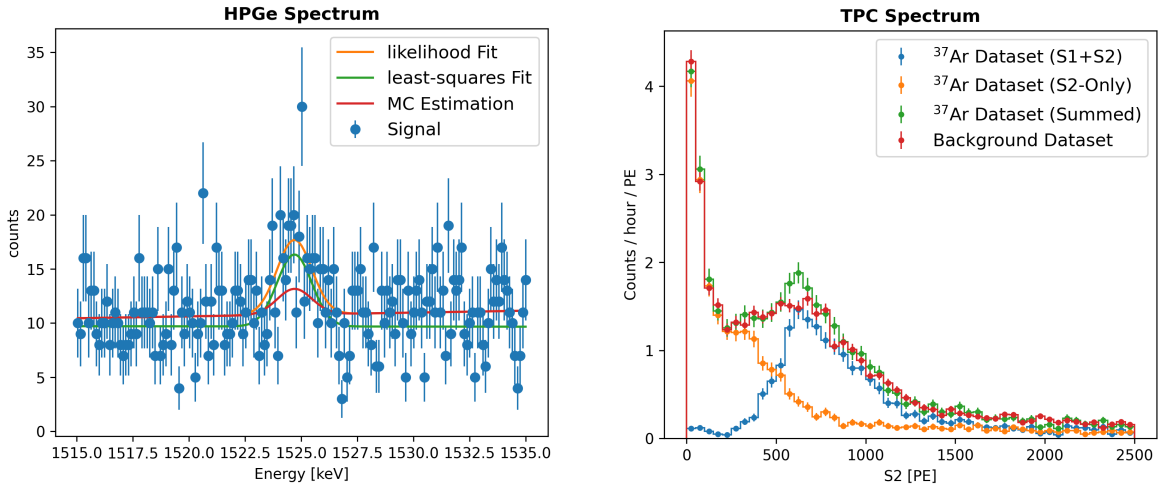


**Figure 4.** The left figure presents the HPGe Spectrum centered on the  $^{42}\text{K}$  peak at 1524.7 keV compared to the MC expectation. The right figure displays the TPC S2 spectrum encompassing the  $^{37}\text{Ar}$  0.27 keV L-shell and the 2.82 keV K-shell radiation peaks.

after  $^{37}\text{Ar}$  injection, as illustrated in figure 4. One can find a tiny excess in the vicinity of 600 PE, which could match the  $^{37}\text{Ar}$  prediction. However, this potential indication could be an artifact of the limit of our system sensitivity to the S1+S2 and S2-Only populations culminating the summed-up observed spectrum shown in green. The background spectrum, in red, represents the summation of the two populations.

## 4 Conclusions

The deployment of the CaO-containing holder to the ReD experiment system through the gas panel was successful; the nano-powder was still intact inside the container and no damage was observed in any of the system components. The successful observation of  $^{42}\text{K}$ , one of the byproducts suggests the success of the activation process of  $^{37}\text{Ar}$ , albeit without precise quantification of its activity since the HPGe measurement is susceptible to some uncertainties. There are some hypotheses for not observing a conclusive evidence for  $^{37}\text{Ar}$ , which include:

- The produced  $^{37}\text{Ar}$  atoms could not liberate nor diffuse out from the matrix because of the nano-powder being damp or because of the powder almost fully filling up the holder.
- The DAQ system configuration is not sensitive enough to such low-energy signal.

Nevertheless, we learnt some lessons for future measurements. This method is reusable and can be done on demand. The CaO nano-powder might have been humid inside the container, which means that pumping was not effective enough, so we might improve by utilizing heating tapes. The ratio between the empty space and the powder-filled space inside the container affects the liberation efficiency significantly. Adjusting the DAQ system and tuning it to trigger on  $^{37}\text{Ar}$  event is not straightforward and needs careful consideration of background rate, signal-to-noise ratio of single PE, dark noise, and the acquisition window.

The stipulated low-energy interval of [0.5, 5] keV assumes paramount significance. By scrutinizing the ionization response within this energy spectrum, the ReD experiment seeks to provide direct measurement of the LAr response to low-energy nuclear recoils. This understanding holds pivotal significance for optimizing the sensitivity of forthcoming experiments such as DarkSide-20k, with the ultimate objective of detecting and scrutinizing particles associated with dark matter.

## Acknowledgments

The speaker acknowledges support from the NCN, Poland (2021/42/E/ST2/00331), the EU's Horizon 2020 (No. 952480, DarkWave project), and IRAP AstroCeNT (Grant No. MAB/2018/7) funded by FNP from ERDF. Acknowledgments are also directed express to the comprehensive technical personnel at INFN Laboratori Nazionali del Sud for their unwavering support throughout the course of this undertaking.

## References

- [1] DEAP collaboration, *Constraints on dark matter-nucleon effective couplings in the presence of kinematically distinct halo substructures using the DEAP-3600 detector*, *Phys. Rev. D* **102** (2020) 082001 [*Erratum ibid.* **105** (2022) 029901] [[arXiv:2005.14667](https://arxiv.org/abs/2005.14667)].
- [2] LUX collaboration, *Results from a search for dark matter in the complete LUX exposure*, *Phys. Rev. Lett.* **118** (2017) 021303 [[arXiv:1608.07648](https://arxiv.org/abs/1608.07648)].
- [3] XENON collaboration, *Dark Matter Search Results from a One Ton-Year Exposure of XENON1T*, *Phys. Rev. Lett.* **121** (2018) 111302 [[arXiv:1805.12562](https://arxiv.org/abs/1805.12562)].
- [4] SUPERCDMS collaboration, *Results from the Super Cryogenic Dark Matter Search Experiment at Soudan*, *Phys. Rev. Lett.* **120** (2018) 061802 [[arXiv:1708.08869](https://arxiv.org/abs/1708.08869)].
- [5] PICO collaboration, *Dark Matter Search Results from the PICO-60 C<sub>3</sub>F<sub>8</sub> Bubble Chamber*, *Phys. Rev. Lett.* **118** (2017) 251301 [[arXiv:1702.07666](https://arxiv.org/abs/1702.07666)].
- [6] GLOBAL ARGON DARK MATTER collaboration, *Sensitivity projections for a dual-phase argon TPC optimized for light dark matter searches through the ionization channel*, *Phys. Rev. D* **107** (2023) 112006 [[arXiv:2209.01177](https://arxiv.org/abs/2209.01177)].
- [7] DARKSIDE collaboration, *Low-Mass Dark Matter Search with the DarkSide-50 Experiment*, *Phys. Rev. Lett.* **121** (2018) 081307 [[arXiv:1802.06994](https://arxiv.org/abs/1802.06994)].
- [8] S. Sangiorgio et al., *First demonstration of a sub-keV electron recoil energy threshold in a liquid argon ionization chamber*, *Nucl. Instrum. Meth. A* **728** (2013) 69 [[arXiv:1301.4290](https://arxiv.org/abs/1301.4290)].
- [9] R. Kishore, R. Collé, S. Katcoff and J.B. Cumming, *<sup>37</sup>Cl(p, n)<sup>37</sup>Ar excitation function up to 24 MeV: Study of (p, n) reactions*, *Phys. Rev. C* **12** (1975) 21.
- [10] R.O. Weber et al., *Cross sections and thermonuclear reaction rates of proton-induced reactions on <sup>37</sup>Cl*, *Nucl. Phys. A* **439** (1985) 176.
- [11] H. Michael, R. Wölfle and S.M. Qaim, *Production of <sup>37</sup>Ar*, *Int. J. Appl. Radiat. Isotopes* **35** (1984) 813.
- [12] C.M. Egnatuk and S.R. Biegalski, *Radioargon production through the irradiation of calcium oxide*, *J. Radioanal. Nucl. Chem.* **298** (2013) 475.
- [13] E.M. Boulton et al., *Calibration of a two-phase xenon time projection chamber with a <sup>37</sup>Ar source*, *2017 JINST* **12** P08004 [[arXiv:1705.08958](https://arxiv.org/abs/1705.08958)].

- [14] D.G. Kelly et al., *The production of Ar-37 using a thermal neutron reactor flux*, *J. Radioanal. Nucl. Chem.* **318** (2018) 279.
- [15] G. Gerbier et al., *NEWS: a new spherical gas detector for very low mass WIMP detection*, [arXiv:1401.7902](https://arxiv.org/abs/1401.7902).
- [16] T.H. Joshi et al., *First measurement of the ionization yield of nuclear recoils in liquid argon*, *Phys. Rev. Lett.* **112** (2014) 171303 [[arXiv:1402.2037](https://arxiv.org/abs/1402.2037)].
- [17] T. Sato et al., *Recent improvements of the particle and heavy ion transport code system — PHITS version 3.33*, *J. Nucl. Sci. Tech.* **61** (2024) 127.